Processing and Application of Ceramics 8 [1] (2014) 7–13
DOI: 10.2298/PAC1401007R

Structural, electrical transport and optical studies of Li ion doped ZnO nanostructures

Rajendran Ajay Rakkesh, Subramanian Balakumar*

National Centre for Nanoscience and Nanotechnology, University of Madras, Maraimalai Campus, Chennai-600025, India

Received 16 February 2014; Received in revised form 20 March 2014; Accepted 23 March 2014

Abstract

In the present work, we studied the morphological aspects, electrical transport and optical properties of pure and lithium ion doped semiconducting ZnO nanostructures successfully prepared by a co-precipitation method. The effect of lithium doping and various morphologies on the structural, electrical and optical properties of these nanostructures were investigated. The X-ray diffraction (XRD) pattern demonstrated that the Li doped ZnO nanostructures exhibits the hexagonal wurtzite structure. A slight change in the 101 peak position was detected among the samples with various morphologies. The UV-Vis diffused reflectance spectroscopic (DRS) studies showed that the band gap increases with Li doping, due to the Burstein-Moss band filling effect. Photoluminescence (PL) studies confirm that the Li incorporation into ZnO material can induce oxygen enrichment of ZnO surface that leads to increase the cyan emission. This material could be used in light emitting diodes in nanoscale optoelectronic devices.

Keywords: *ZnO nanostructures, photoluminescence, cyan emission, Burstein-Moss shift*

I. Introduction

Zinc oxide is a direct-band-gap semiconducting material with an energy gap of 3.3 eV at room temperature. It has higher excitation binding energy and good optical property at room temperature. ZnO is a very attractive and promising material for low-voltage and short-wavelength electro-optical devices such as light emitting diodes and laser diodes; its other applications comprise transparent ultraviolet protection films, gas sensors and varistors [1–6]. Recently, considerable attention has been focused on ZnO low-dimensional materials such as nanorods, nanowires and nanobelts [7,8]. There are a number of techniques for preparing nano-sized ZnO materials. However, it is still attractive to find a simple method to synthesize ZnO nanomaterials. The electronic band structure and its optimization are of great importance in designing semiconductor devices and it can be simulated by changing the material crystal structure and chemical composition. As the impurity atoms are introduced, the spatial geometries which are providing the lowest energy configuration in the bulk may not provide the same as when the surface atoms and surface bonds are altered. Such modifications are much more important in many electronic and optoelectronic devices, especially illustrated in injection lasers and bipolar transistors [9]. Theoretically and experimentally, the importance of dopants and their influence on optical and transport properties are evaluated. To achieve stable p-type ZnO semiconductor, dopants from I and V group elements are introduced and their property studies including structure, morphology, optical, magnetic and transport properties are updated periodically [10–12]. It is said in few citations that the addition of lithium tremendously increases the electrical resistivity and hence is applied to transparent conducting oxides (TCO) electrodes, piezoelectric devices and memory devices [13–15].

The present work was undertaken to access the effect of Li doping influence on the morphological, electrical and optical properties of ZnO nanomaterials. The as-synthesized nanomaterials were characterized by X-ray diffractometer (XRD), field emission scanning electron microscope (FESEM), UV-Vis diffused reflectance spectroscopy (DRS) and photoluminescence

* Corresponding author: tel: +91 44 22202749,
fax: +91 44 22352494, e-mail: *balasuga@yahoo.com*

(PL) spectroscopy. Further, the formation mechanism from nanospheres to nanorods was proposed. The detailed investigation of the cyan light emitting Li doped ZnO nanostructures is discussed.

II. Experimental details

2.1. Materials

Zinc acetate dehydrate was procured from Merck chemical companies and lithium hydroxide was bought from the Sisco chemical laboratory. All chemicals used in this work are analytical grade and used without further purification. All solutions were prepared from doubly distilled water obtained from in-house developed water purification system.

2.2. Methods

An aqueous solution containing a mixture of zinc acetate and lithium hydroxide in an appropriate amount of $Zn_{1-x}Li_xO$ (x = 0, 0.05 and 0.10 mol) is used to synthesize pure and Li doped ZnO nanomaterial without any expensive surfactants. The aqueous solution was kept in a magnetic stirrer for 4 h. The white precipitate was obtained by washing and filtered with ethanol and water solution. Finally, the filtered product was annealed in a muffle furnace at 350 °C for 2 h.

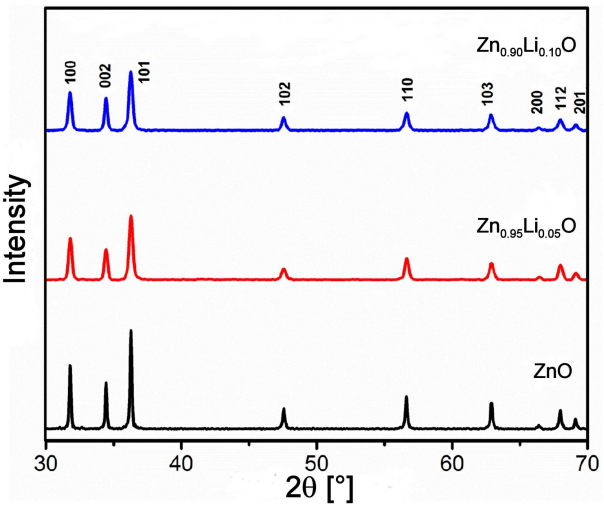

Figure 1. X-ray diffraction pattern of $Zn_{1-x}Li_xO$ (x = 0, 0.05 and 0.10 mol) nanomaterials

2.3. Materials characterization

The morphology and structure of the as-prepared pure and Li doped ZnO nanomaterial samples were characterized using the field emission scanning electron microscopy (FESEM) (Hitachi SU 6600) and X-ray diffraction (XRD) (PANalytical with CuKα1 of 1.5406 Å). The band gap of the materials was analysed by UV-Vis DRS spectroscopy (Perkin Elmer Lambda 650). The photoluminescence (PL) spectrum was recorded by a Perkin Elmer MPF-44B equipped with 150 W xenon lamp under (325.0 nm) excitation.

III. Results and discussion

3.1. Phase analysis

Figure 1 shows the XRD profile of the pure and lithium-doped ZnO nanomaterials with different dopant concentrations. All the diffraction peaks are well indexed with pure hexagonal phase of wurtzite structure, and the phase remains unaltered even with the increase in dopant content from 0 to 0.10 mol. The assigned peak is made by comparing with the standard JCPDS data (Card ID-36-1451). By doping with lithium, the dopant atoms occupy the Zn sites in the ZnO lattice as their ionic radii are comparable [16].

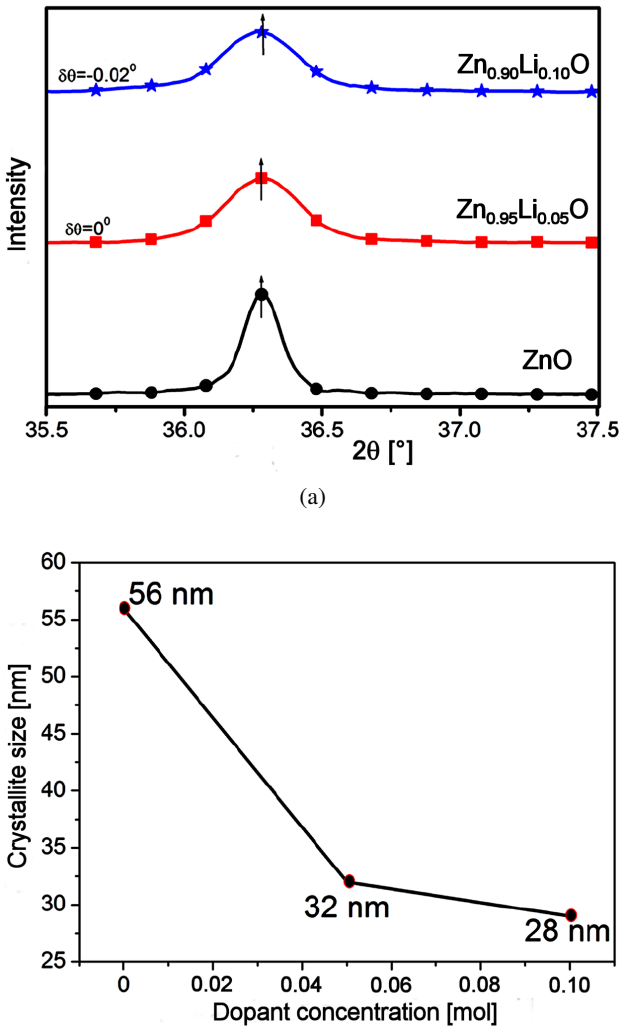

Figure 2. Changes in the 101 wurtzite peak position (a) and crystallite size with lithium concentration (b)

The average crystallite sizes of the entire as-synthesized lithium-doped sample are calculated using Scherrer equation. For this, the characteristic 101 peak of ZnO at 2θ = 36.28° and their full width at half maximum (FWHM) are considered by using the Cauchy Loretzian fit. The average crystallite size of the pure ZnO is calculated to be 56 nm. As the dopant con-

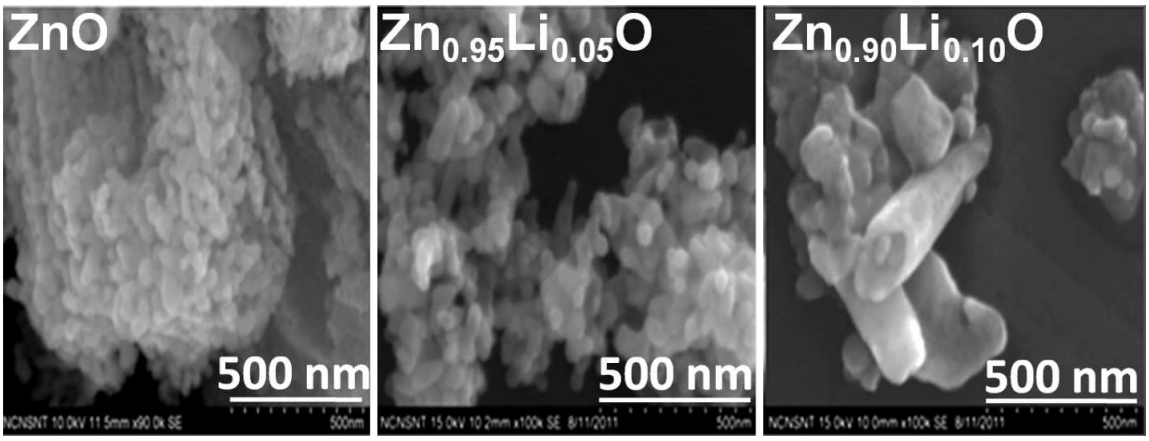

(a) (b) (c)

Figure 3. FESEM micrographs of wet chemically grown nanoparticles: a) undoped ZnO, b) 0.05 mol lithium doped ZnO and c) 0.10 mol lithium doped ZnO

tent has increased from 0, 0.05 to 0.10 mol of lithium, there is a regular decrease in crystallite size from 56, 32 and 28 nm, respectively; explaining the incorporation of dopant atom inhibits the growth of the ZnO nanomaterials. The lattice distortion and decrease in crystallite size are denoted in terms of peak shift and peak width. At a low carrier concentration, the peak position at 101 has a 2θ value is 36.28, while at higher concentration, the peak position of 101 plane has decreased to 36.26 degrees. The broadening of the 101 peak can be highly confined and localized in the ZnO lattice fluctuation. This random potential fluctuation due to redistribution, rearrangement of surface atoms and alteration of surface bonding, shift the 101 peak position accordingly. The shift in peak position, doping concentration dependent crystallite size variation and the calculated value of $\delta\theta$ were represented in Fig. 2 with respect to the pure ZnO.

3.2. *Morphological analysis*

Particle size distribution and direct images of the pure and Li doped ZnO nanomaterials were imaged from FE-SEM micrographs. Figure 3 shows the high magnified (90.000× and 100.000×) FESEM micrographs of the pure, 0.05 and 0.10 mol Li-doped ZnO nanomaterials. It can be observed that the morphology and particle size are different with respect to doping. The image of the pure ZnO nanomaterials sample indicates the formation of nanosphere bundles. In the case of 0.05 mol lithium-doped ZnO, the nanoparticles are spherical in nature with a high degree of agglomeration and aggregation. It can be concluded that the morphology of 0.10 mol lithium-doped ZnO is a rod-like structure with non-uniform size distribution. The individual nanorods have a length of about 500 nm and diameter of about 175 nm. The nanorods are long with blunt end resembling a hexagonal surface. Thus, when the ZnO nanomaterials are doped with lithium atoms there is a morphology evolution from spherical to rod-like nature. The incorporation of lithium inhibits the rate of particle growth, but promotes the rate of nucleation, thus producing large number of particles in the given co-precipitation reaction period.

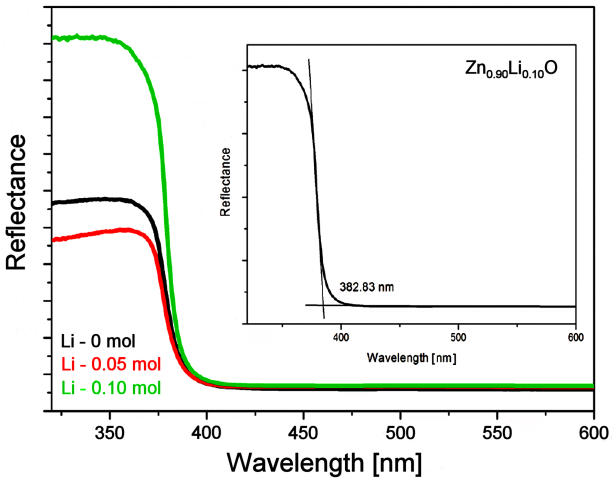

Figure 4. UV diffused reflectance spectra of $Zn_{1-x}Li_xO$ (x = 0, 0.05 and 0.10 mol). The insert shows the point of intersection, measured in Li 10 mol doped ZnO

3.3. *Band gap widening*

The UV-Vis diffused reflectance spectra of the pure and Li doped ZnO nanostructures as a function of wavelength are shown in Fig. 4 and the inset picture shows the method adopted to mark the onset of reflectance for the sample with 0.10 mol Li. It is shown experimentally that an increase in hole concentration, the onset of reflectance and the spectrum maximum are shifted towards the lower wavelength region. There is a significant change in the amount of reflectance due to the introduction of lithium atom into ZnO lattice. In the lithium-doped ZnO nanoparticles, the UV-Vis spectroscopy is blue-shifted by 10 nm (392–382 nm), due to widening of the band gap (Fig. 5). For the direct transition, the optical band gap energy of the lithium-doped

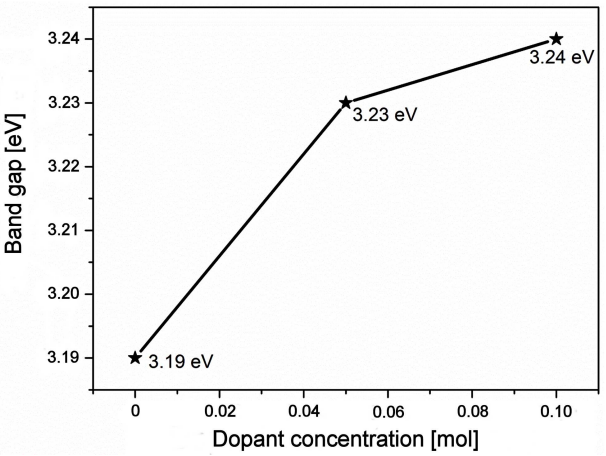

Figure 5. Variation in the optical band gap with an increase in dopant amount

ZnO nanoparticles is determined using the Tauc plot relation $\alpha h\nu = C(h\nu - E_g)^{1/2}$ where $h\nu$ is the photon energy in eV, E_g is the optical band gap in eV and C is the constant [17]. The direct band gap is determined by extrapolating and intersecting the linear portion of $(\alpha h\nu)^2$ to the energy axis $h\nu = 0$ (shows in inset of Fig. 4). From the graph, the calculated band gap energy of the undoped and doped ZnO comes out to be 3.19, 3.23, 3.24 eV for the pure ZnO, 0.05 mol Li doped ZnO and 0.10 mol Li doped ZnO, respectively. The observed blue shift in the wavelength is the reflection of the band gap widening, owing to the quantum size effect (QSE) [18,19]. However, the QSE is highly evident only when the crystallite size of the nanocrystalline ZnO semiconductor is comparable to its Bohr exciton radius. But, the crystallite sizes of the Li doped ZnO obtained from XRD is far beyond the quantum confinement regime. Accordingly, the shift in reflectance edge and widening of the band gap can be determined on the basis of Burstein-Moss shift and it is well pronounced in highly doped semiconductor [20]. Since, the Li doped ZnO samples are degenerate p-type semiconductors, the Fermi level lies in the valence band, and their position depends on the hole concentrations. Thus, the optical band gap of the materials calculated from UV diffused reflectance is related to the excitation of the electrons from the Fermi level in the valence band to the conduction band. The increase in the optical band gap energy to the increase of dopant concentration is attributed to the Burstein-Moss effect [20]. In the lithium-doped ZnO nanomaterials, when maximum numbers of free carrier holes are added, the topmost electronic states in valence band become vacant and, hence, shift the reflectance edge towards higher photon energy. The shift in Fermi energy level prohibits the interband transition through Pauli's exclusion principle [21].

Figure 6 easily demonstrates the overall band gap widening mechanism involved in lithium-doped ZnO nanostructures. In a *p-type semiconductor*, the Fermi energy level lies close to the valence band. As the free carrier concentration (hole) adds up while doping with lithium atom, the position of Fermi level gets disturbed and shifted within the valence band. Due to the incorporation of holes or a vacant energy state, the electrons in the valence band make a transition to occupy the available states. This transition and the gradual addition of holes make the Fermi level to shift further below the valence band and thus widen the band gap [20].

3.4. Photoluminescence spectroscopic analysis

The optical properties of the pure and Li doped ZnO nanostructures were investigated by photoluminescence (PL) spectroscopy. To investigate the effects of Li doping and defect-mediated emission by optimize the relative change in the intensity. The PL spectra were obtained for the pure ZnO, 0.05 mol Li doped ZnO and 0.10 mol Li doped ZnO nanostructures. In the emission spectra three different regions can be seen: the ultraviolet (P1: ~350 to 450 nm), blue (P2: ~380 to 500 nm) and green (P3: ~480 to 600 nm) regions, as shown in Fig. 4.

The blue emission and green emission have been reported to arise from Zn ions at interstitial sites (Zn_i) of ZnO nanocrystalline materials [22,23], and oxygen vacancy (V_O) [24,25], respectively. These emissions are confirmed in the spectra of the pure ZnO sample (Fig. 7). On the other hand, the cyan emission at 465 nm is commonly attributed to excess oxygen on the ZnO surface. By increasing the Li doping from 0.05 to 0.10 mol, the relative intensity of the cyan emission increases gradually. It may be due to both Li_{Zn} and Li_i in the ZnO nanocrystalline material. The transitions from donor levels in the crystal (can be both from V_O or Li_i) to Li_{Zn} acceptor levels release cyan emissions. At 0.05 mol doping, the peaks of the native defects (Zn_i and V_O) of ZnO remain relatively unchanged. Thus, the change in the cyan emission intensity confirms the replacement of Zn by the smaller Li atom in the crystal. This is supported by the decrease ZnO crystallite size as observed by XRD analysis (Fig. 2). On the other hand, at 0.10 mol doping, the UV emission of the nanocrystalline material significantly decreased and the cyan emission continued to increase. This indicates the reduction of V_O and a proliferation of Li impurity in the crystal. Li ions cannot substitute for O (Li_O) in the crystal lattice due to the high formation energy [26]. The Li ions can diffuse into the spaces in between the lattice (Li interstitial, Li_i). The diffusion of Li_i leads to an increase in both crystallite size and lattice parameter as seen in Fig. 2. Interestingly, the cyan emission band, which relates to excess oxygen at the surface, becomes stronger as the doping content is increased to 0.10 mol Li. We believe that Li incorporation into ZnO can induce oxygen-enrichment of ZnO surfaces that leads to increase the cyan emission [27,28].

IV. Conclusions

In summary, lithium doped zinc oxide nanostructures have been successfully prepared using co-precipitation method. The nanostructures are crystalline with a wurt-

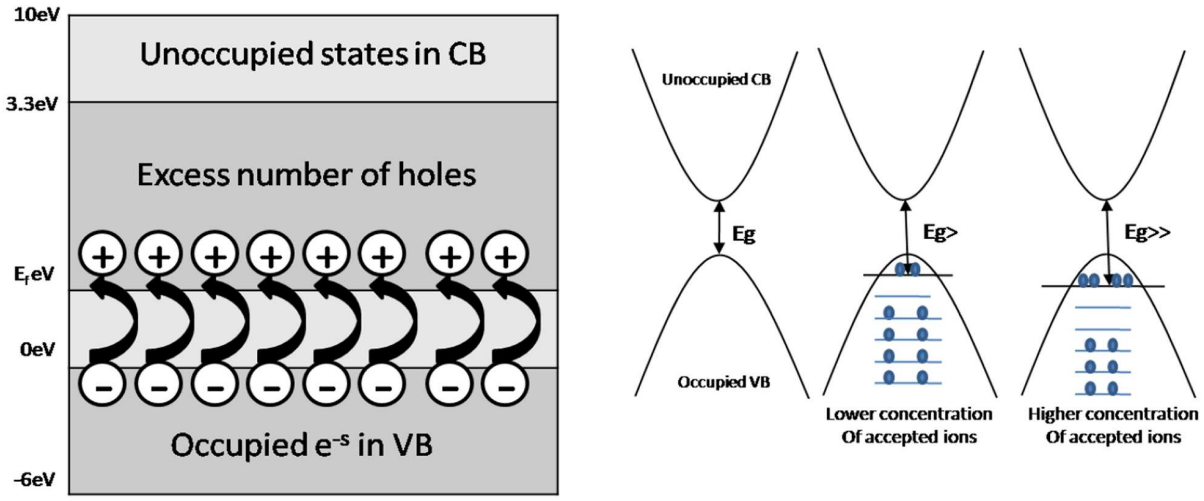

Figure 6. Schematic illustration of the Burstein-Moss shift in lithium-doped ZnO nanoparticles

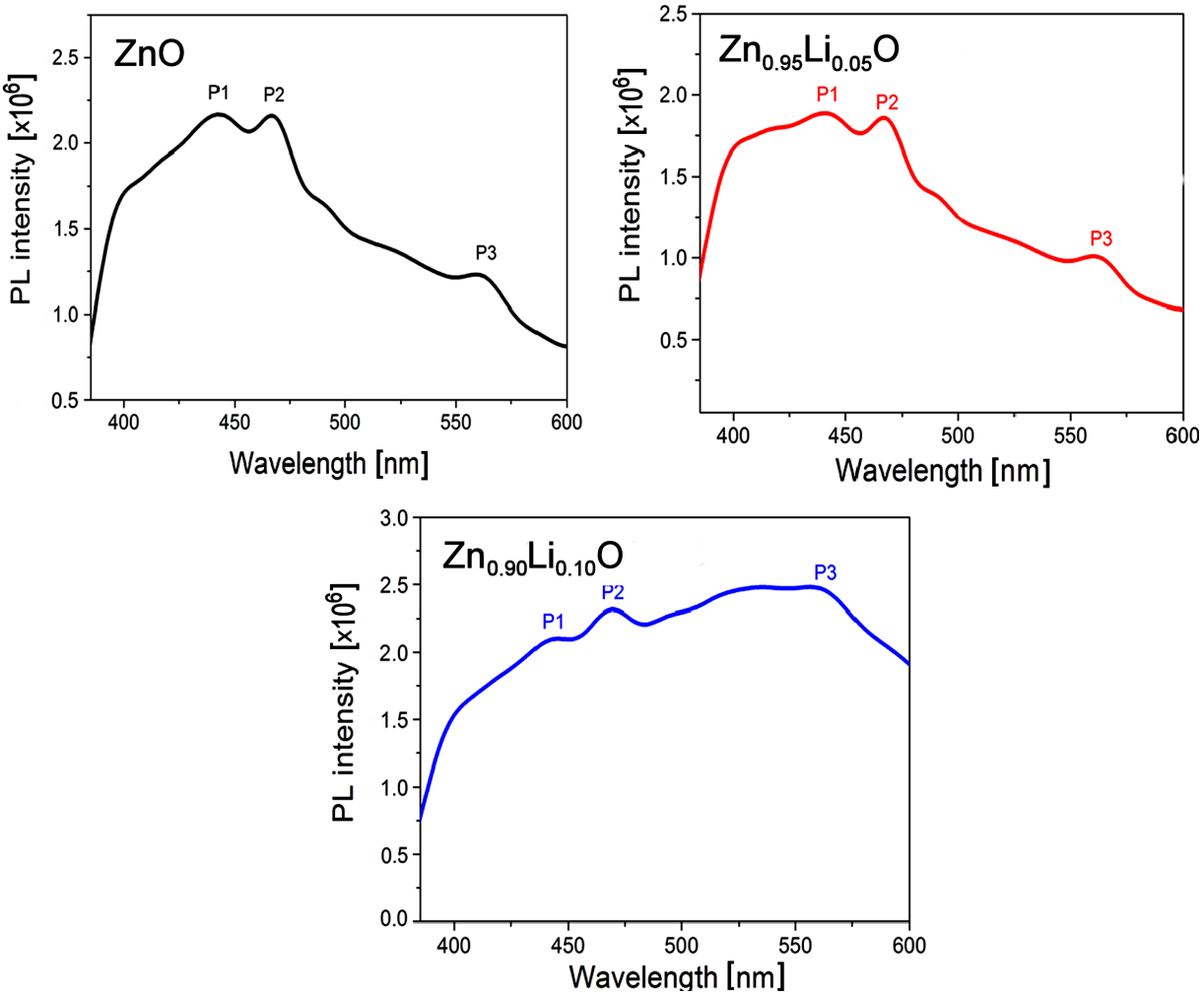

Figure 7. Room temperature photoluminescence spectra for $Zn_{1-x}Li_xO$ (x = 0, 0.05 and 0.10 mol): P1-P3 denotes the ultraviolet emission, blue emission and green emission, respectively

zite structure. The electronic band gap and photoluminescence intensity of the nanostructure increases, while increasing the lithium concentration. The PL spectra at room temperature showed the cyan emission at 465 nm. The cyan emission bands are attributed to Li incorporation into ZnO that can induce oxygen-enrichment on the surfaces leading to the increase of the cyan emission. We believe that these nanostructures could be used as light-emitting devices in nanoscale optoelectronic applications.

Acknowledgement: R. Ajay Rakkesh acknowledges the University of Madras for providing NCNSNT fellowship to carry out this research work.

References

1. J. Yu, X. Yu, "Hydrothermal synthesis and photocatalytic activity of zinc oxide hollow spheres", *Environ. Sci. Technol.*, **42** (2008) 4902–4907.
2. Z. Fan, J.G. Lu, "Nanostructured ZnO: Building blocks for nanoscale devices", *Int. J. High Speed Electron. Syst.*, **16** (2006) 883–886.
3. O. Lupan, G. Chai, L. Chow, "Novel hydrogen gas sensor based on single ZnO nanorod", *Microelectron. Eng.*, **85** (2008) 2220–2225.
4. E. Galoppini, J. Rochford, H. Chen, G. Saraf, Y. Lu, A. Hagfeldt, G. Boschloo, "Fast electron transport in metal organic vapour deposition grown dye sensitized ZnO nanorod solar cells", *J. Phys. Chem. B*, **110** (2006) 16159–16161.
5. B.S. Ong, C. Li, Y. Li, Y. Wu, R. Loutfy, "Stable, solution processed high-mobility ZnO thin film transistor", *J. Am. Chem. Soc.*, **129** (2007) 2750–2751.
6. R. Konenkamp, R. Word, C. Schlegel, "Vertical nanowire light emitting diode", *Appl. Phys. Lett.*, **85** (2004) 6004.
7. Z.L. Wang, *Nanowires and Nanobelts: Materials, Properties and Devices.*, Kluwer Academic Publishers, Netherlands, 2003.
8. Y. Li, F. Qian, X. Xiang, C.M. Lieber, "Nanowire electronic and optoelectronic devices", *Mater. Today*, **9** [10] (2006) 18–27.
9. J.C. Johnson, H. Yan, P. Yang, R.J. Saykally, "Optical cavity effects in ZnO nanowire lasers and waveguides", *J. Phys. Chem. B*, **107** (2003) 8816–8828.
10. G.D. Yuan, W.J. Zhang, J.S. Jie, X. Fan, J.A. Zapein, Y.H. Leung, L.B. Luo, P.F. Wang, C.S. Lee, S.T. Lee, "p-type ZnO nanowire arrays", *Nano Lett.*, **8** (2008) 2591–2597.
11. Y. Miao, Z. Ye, W. Xu, F. Chen, X. Zhou, B. Zhao, L. Zhu, J.G. Lu,"p-type conduction in phosphorus-doped ZnO thin films by MOCVD and thermal activation of the dopant", *Appl. Surf. Sci.*, **252** (2006) 7953–7956.
12. T. Aoki, Y. Shimizu, A. Miyake, A. Nakamura, Y. Nakanishi, Y. Hatanaka, "p-type ZnO layer formation by excimer laser doping", *Phys. Status Solidi B*, **229** (2002) 911–914.
13. H.J. Xiang, J. Yang, J.G. Hou, Q. Zhu, "Piezoelectricity in ZnO nanowires: A first-principles study", *Appl. Phys. Lett.*, **89** (2006) 223111.
14. K. Ellmer, R. Mientus, "Carrier transport in polycrystalline transparent conductive oxides: A comparative study of zinc oxide and indium oxide", *Thin Solid Films*, **516** (2008) 4620–4627.
15. B. Yi, C.C. Lim, G.Z. Xing, H.M. Fan, L.H. Van, S.L. Huang, K.S. Yang, X.L. Huang, X.B. Qin, B.Y. Wang, T. Wu, L. Wang, H.T. Zhang, X.Y. Gao, T. Liu, A.T.S. Wee, Y.P. Feng, J. Ding, "Ferromagnetism in dilute magnetic semiconductors through defect engineering: Li-doped ZnO", *Phys. Rev. Lett.*, **104** (2010) 137201.
16. Y.J. Lina, M.S. Wangb, C.J. Liub, H.J. Huanga, "Defects, stress and abnormal shift of the (002) diffraction peak for Li-doped ZnO films", *Appl. Surf. Sci.*, **256** (2010) 7623–7627.
17. X.B. Lou, H.L. Shen, H. Zhang, "Optical properties of nanosized ZnO films prepared by sol-gel process", *Trans. of Nonferr. Metals Soc. China*, **17** (2007) 814–817.
18. S. Fuvukawa, T. Myasato, "Quantum size effects on the optical band gap of microcrystalline Si:H", *Phys. Rev. B*, **38** (1988) 5726.
19. M.K. Lee, H.F. Tu, "Ultraviolet emission blueshift of ZnO related to Zn", *J. App. Phys.*, **101** (2007) 126103.
20. P.D.C. King, T.D. Veal, F. Fuchs, C.Y. Wang, D.J. Payne, A. Bourlange, H. Zhang, G.R. Bell, V. Cimalla, O. Ambacher, R.G. Egdell, F. Bechstedt, C.F. McConville, "Band gap, electronic structure, and surface electron accumulation of cubic and hombohedral In_2O_3", *Phys. Rev. B*, **79** (2009) 205211.
21. M. Fox, "Optical properties of solids", pp. 50 in *Oxford Master Series in Condensed Matter Physics*, New York, 2003.
22. M.K. Patra, K. Manzoor, M. Manoth, S.R. Vadera, N. Kumar, "Studies of luminescence properties of ZnO and ZnO:Zn nanorods prepared by solution growth technique", *J. Lumin.*, **128** (2008) 267–272.
23. D.H. Zhang, Z.Y. Xue, Q.P. Wang, "The mechanisms of blue emission from ZnO films deposited on glass substrate by r.f. magnetron sputtering", *J. Phys. D: Appl. Phys.*, **35** (2002) 2837.
24. B. Panigrahy, M. Aslam, D.S. Misra, M. Ghosh, D. Bahadur, "Defect-related emissions and magnetization properties of ZnO nanorods", *Adv. Funct. Mater.*, **20** (2010) 1161–1165.
25. K. Vanheusden, C.H. Seager, W.L. Warren, D.R. Ta-

llant, J.A. Voigt, "Correlation between photoluminescence and oxygen vacancies in ZnO phosphors", *Appl. Phys. Lett.*, **68** (1996) 403.

26. N. Ohashi, T. Nakata, T. Sekiguchi, H. Hosono, M. Mizuguchi, T. Tsurumi, J. Tanaka, H. Haneda, "Yellow emission from zinc oxide giving an electron spin resonance signal at $g = 1.96$", *Jpn. J. Appl. Phys.*, **38** (1999) L113–L115.
27. V.A. Funobevov, K.A. Alim, A.A. Balandin, "Photoluminescence investigation of the carrier recombination processes in ZnO quantum dots and nanocrystals", *Phys. Rev. B*, **73** (2006) 165317.
28. J.B. Kim, D. Byun, S.Y. Ie, D.H. Park, W.K. Choi, J.W. Choi, B. Angadi, "Cu-doped ZnO-based p-n hetero-junction light emitting diode", *Semicond. Sci. Technol.*, **23** (2008) 095004.